Biomass Conversion and Biorefinery (2024) 14:2799–2818
https://doi.org/10.1007/s13399-022-02493-2

ORIGINAL ARTICLE

Catalytic pyrolysis of date palm seeds on HZSM-5 and dolomite in a pyroprobe reactor in line with GC/MS

Miriam Arabiourrutia[1] · Gmar Bensidhom[2] · Maider Bolaños[1] · Aïda Ben Hassen Trabelsi[2] · Martin Olazar[1]

Received: 6 December 2021 / Revised: 9 February 2022 / Accepted: 19 February 2022 / Published online: 11 March 2022

Abstract
Catalytic pyrolysis of date palm seeds (DPS) has been carried out in a pyroprobe connected online with a GC/MS. The effect of a HZSM-5 zeolite on the product distribution has been studied at 450 and 500 °C by using different catalyst/biomass mass ratios (1, 2, 5) and that of a dolomite catalyst at 450 °C using a catalyst/biomass mass ratio of one. Product distributions have been monitored and their trends explained based on the properties of the catalysts used. The HZSM-5 promotes the formation of incondensable gases and aromatic hydrocarbons due to its high acidity and shape selectivity. The concentrations of incondensable gases and hydrocarbons increase markedly with the catalyst/biomass mass ratio, with their peak area percentages ranging from 23.6 to 54.1% and from 7.1 to 24.5%, respectively. At the same time, a significative reduction in the amount of acids, ketones, phenols, furans, and anhydrosugars has been determined. The dolomite catalyst enhances ketonization reactions, which leads to a significant increase in the content of ketones, accounting for a value of around 27%.

Keywords DPS biomass · Py-GC/MS · Catalytic pyrolysis · Zeolite HZSM-5 · Dolomite

1 Introduction

Biomass is a renewable energy source, which may be used to replace fossil fuels, and so meet the increasing energy demand. Pyrolysis of biomass is an interesting option to manage forestry and agricultural wastes and, at the same time, obtain products with a high potential application for energy production or source of value-added chemicals contained in the gaseous and/or liquid bio-oil fraction [1, 2].

The bio-oil or pyrolytic oil generated from the fast pyrolysis of biomass and wastes may have several potential applications, such as those related to the production of high value-added chemicals and substitutes of petroleum-based sources for a wide range of fuels [3]. Crude bio-oil derived from the conventional fast pyrolysis is a low-grade liquid fuel due to the high oxygen content, poor stability, high acidity, and low calorific value. Furthermore, recovery of valuable chemicals is a very difficult task due to their low contents in the bio-oil. Accordingly, the liquid product must be upgraded prior to use in relevant applications by means of suitable processes, such as catalytic cracking, which in turn must involve reasonable costs.

Catalytic fast pyrolysis is considered a promising approach to convert oxygenate compounds into a variety of hydrocarbons and therefore improve the bio-oil quality. The use of a catalyst generally enhances the targeted reactions; reduces the reaction time and temperature; improves the liquid oil quality by removing oxygen via certain reactions, such as dehydration (removing oxygen as H_2O), decarboxylation (removing oxygen as CO_2), and decarbonylation (removing oxygen as CO) [4, 5]; and increases the overall process efficiency [6]. The surface area, acidity, and pore size and volume are the key features of any catalyst affecting the pyrolysis process [7].

There are many studies in the literature dealing with the catalytic pyrolysis of biomass and wastes as a way to obtain upgraded pyrolytic products [8, 9]. Thus, acid catalysts such as HZSM-5 zeolite-based ones have been reported to perform well in deoxygenation to obtain hydrocarbons.

✉ Miriam Arabiourrutia
miriam.arabiourrutia@ehu.eus

[1] Department of Chemical Engineering, University of the Basque Country UPV/EHU, P.O. Box 644, E48080 Bilbao, Spain

[2] Centre de Recherches et des Technologies de l'Energie Technopole De Borj-C´edria, BP: 95, Hamam Lif, Ben Arous, Tunisia

This behavior has been attributed to their acidity and shape selectivity [5, 10], with the latter being a consequence of its small/medium-pore size coupled with its two-dimensional channel-like pore system [11]. In the pyrolysis of biomass, deoxygenation of holocellulose and lignin fragments occurs via dehydration and decarbonylation/decarboxylation reactions [12, 13]. Subsequently, protolytic cracking or β-scission, alkylation, isomerization, cyclization, oligomerization, and aromatization reactions take place. Among the zeolites, the ZSM-5 has been widely used as a catalyst for biomass pyrolysis, as it dramatically changes the composition of the volatiles generated. One of the main purposes of using zeolitic catalysts lies in its capacity for deoxygenating phenolic and oxygenated compounds [14]. Other catalysts, such as alkali salts [15] and metal oxides [16], have been used, but a much lower deoxygenating activity has been reported. Low-cost catalysts, either natural (olivine, alumina) or synthetic (spent FCC catalyst), have also been used in line with the pyrolysis reactor, and they led to a significant decrease in acid and phenolic compounds in the volatile stream, making it suitable for further catalytic valorization for the production of H_2, fuels, and chemicals [17]. Other studies in which natural materials have been used as catalysts are those by Aljbour [18] and Aljeradat et al. [19].

Dolomite is a natural, inexpensive, and non-metallic catalyst, which has been widely used for tar conversion in biomass gasification [20, 21]. However, this natural catalyst has also been used successfully in the catalytic pyrolysis of biomass to improve the bio-oil quality by cracking heavy organic molecules to lighter ones or removing oxygen from the oxygenates [22]. Furthermore, this catalyst has also been used to upgrade the liquid bio-oil prior to feeding into the reforming reactor. Thus, Valle et al. [23] concluded that dolomite was effective for the deoxygenation of the bio-oil, as it reduces the O content, and so the O/C ratio, in the upgraded bio-oil. Ly et al. [22] used dolomite as a catalyst in a fluidized bed and proved that it leads to the formation of aromatic compounds (C_5-C_{11}), such as the derivatives of furfural, ketones, and phenolic compounds. Another positive benefit of dolomite lies in its capacity for CO_2 capture, which allows obtaining a gaseous product with a low yield of CO_2 [24]. Dolomite removes oxygen from the pyrolysis stream mostly through dehydration, instead of decarboxylation or decarbonylation [22].

In this work, date palm seeds have been used as the raw material. The date palm tree is a typical cultivated tree in the arid and semi-arid regions of the world. There are more than 100–120 million date palm trees worldwide, with most of them (70–90%) being located in the Middle East and North Africa (MENA) countries [25]. It is especially abundant in several regions in the South of Tunisia [26].

Date seeds are low-cost agricultural by-products, which are traditionally used for animal feed. Their derived powder is used as a coffee substitute [27, 28]. They are also used as a source of oil in cosmetics due to their antioxidant properties, raw material for activated carbon, adsorbent for dye-containing waters, and CO_2 capture material [29–31]. The annual world production of dates is of around 9 million tons [29]. Depending on the variety, date seeds account for 6.10–11.4% of the whole fruit weight [32].

This study analyzes the performance of a HZSM-5 zeolite catalyst by varying temperatures (450 and 500 °C) at the catalyst/biomass mass ratio of C/B=1 and catalyst/biomass mass ratio (C/B=1, 2, and 5) at the temperature of 450 °C. A detailed quantification and identification of the compounds formed have been carried out, with emphasis placing on the different trends observed in the product distribution and relating these trends to the properties of the catalysts used. Furthermore, a low-cost natural catalyst with very different properties, as is dolomite, has been used to analyze its effect on the product distribution and compare its performance with that of the HZSM-5. The aim of this study is to show that upgrading of the condensable fraction (bio-oil) allows improving the quality of the liquid and therefore increases its potential for use as fuel. In fact, the presence of aliphatic and aromatic hydrocarbons in the liquid is crucial for a high-quality fuel. Furthermore, it is well-known that catalytic pyrolysis enhances the production of hydrocarbons. To our knowledge, there are no studies reported in the literature about the catalytic pyrolysis of date palm seeds. Therefore, this study contributes to promoting pyrolysis processes as an option to valorize these wastes.

2 Experimental

2.1 Preparation and characterization of date palm seed samples

Date palm seeds (DPS) were supplied by the National Institute of Arid Zone (IRA-Kebili, Tunisia). The sort of date used was Deglet Noor seeds (*Phoenix Dactylifera L.*). The DPS were harvested from the date fruit by hand and then cleaned with distilled water to eliminate all dust. They were then sundried for 3 days. Moreover, the sundried biomass was crushed into particle sizes ranging between 0.125 and 0.25 mm and stored in airtight plastic bags to prevent moisture absorption. This particle size range is the suitable one to carry out fast pyrolysis in a Py-GCMS, where very small quantities of sample are used, of around 1 mg.

A thermogravimetric analyzer (TGA Q5000 IR) was used in this study to determine the proximate analysis of the DPS samples. The procedure was described elsewhere [33].

DPS ultimate analysis was performed using an elemental analyzer (LECO CHNS TRuSpec). The O content was determined by difference, according to the following expression:

$$O\ (wt.\%) = 100 - \left[C\ (wt.\%) + H\ (wt.\%) + N\ (wt.\%)\right.$$

The higher heating value (HHV) of the raw material DPS was measured by means of a CAL-2 K Oxygen Bomb Calorimeter according to the ASTM D5865-13 standard method.

The lignocellulosic components (cellulose, hemicellulose, and lignin) of the DPS sample were determined according to the method described elsewhere [34].

2.2 Py-GC/MS equipment

The pyrolysis of DPS has been carried out in a Pyroprobe 5150 of CDS. One milligram of the sample was inserted in the pyrolysis tube, with quartz wool being placed above and below the sample. Pyrolysis runs were carried out at 450 and 500 °C for 40 s. This time is sufficiently long to ensure all the volatile matter is pyrolized. The experiments were conducted in triplicate and the mean values and the standard deviations were determined. In the catalytic pyrolysis, the biomass sample was mixed with the catalyst at the catalyst/biomass (C/B) mass ratios of 1, 2, and 5 for the HZSM-5 zeolite and 1 for the dolomite catalyst. The heating rate was 20 °C/ms. The volatiles generated were transferred through a hot line into a GC/MS (QP2010 Shimadzu), where they were analyzed. The chromatographic separation was performed using a BPX-5 capillary column (30 m × 0.22 mm ID, 0.25 µm film thickness). The oven temperature was programmed from 45 °C (maintained for 3 min) to 295 °C (5 min) with a heating rate of 4 °C/min. The MS detector was a quadrupole type. The identification of the compounds was carried out using the NIST library.

2.3 Catalysts

The catalysts used are a HZSM-5 zeolite and a dolomite. The HZSM-5 zeolite has been chosen because of its good deoxygenation capacity given by its specific properties (acidity and shape selectivity). The dolomite catalyst has been chosen because of, on the one hand, low cost and, on the other hand, different properties to those of the zeolite, e.g., poor porous structure and basic nature.

The ZSM-5 zeolite has been supplied by Zeolyst International (USA) and the dolomite by Minerals Sibelco (Spain).

The ZSM-5 zeolite was supplied in ammoniac form and calcined at 575 °C for 2 h in order to obtain the acid form and so a suitable surface acidity. The dolomite has been calcined at 900 °C for 4 h in order to attain full decarboxylation of calcium and magnesium carbonates and so obtain the active phases of CaO and MgO. XRD analysis has been carried out to determine the crystalline phases in the dolomite. The crystalline structure of the dolomite was analyzed using X-ray powder diffraction (XRD) patterns. A Bruker D8 Advance diffractometer with Cu Kα1 radiation was used to conduct the analysis. XRF analysis has been carried out to measure the chemical composition of the catalyst. This analysis was carried out using a sequential wavelength dispersion X-ray fluorescence (WDXRF) spectrometer (Axios 2005, PANalytical) under a vacuum atmosphere.

The textural properties of both catalysts have been determined from the N_2 adsorption-desorption curves obtained in a *Micromeritics ASAP-2100* equipment. The total acidity of the HZSM-5 zeolite has been determined in a calorimeter (*Setaram TG-DSC 111*) coupled to a mass spectrometer (*Thermostar* of *Balzers Instruments*).

3 Results

3.1 Biomass characterization

Table 1 shows the proximate and ultimate analyses of the studied DPS sample, as well as the percentages of their main constituents (cellulose, hemicellulose, and lignin).

Date seeds are characterized by their high content of volatile matter and low one of ash components. High volatility makes these biomasses attractive for the pyrolysis process in order to obtain bio-oil and syngas [35].

3.2 Catalyst characterization

Table 2 sets out the physicochemical properties of the HZSM-5 zeolite and dolomite catalysts. As observed, the zeolite has much higher surface area and pore volume than the dolomite, whereas the average pore size of the dolomite is much higher than that of the zeolite. The latter is evidence of the microporous structure of the zeolite. Concerning acidity, the zeolite is an acid catalyst, whereas

Table 1 Ultimate and proximate analyses and lignocellulosic components of the studied DPS

Proximate analysis	
Moisture content (wt.%)	1.73
Volatile matter content (wt.%)	78.61
Ash content (wt.%)	4.97
Fixed carbon* (wt.%)	14.69
Ultimate analysis	
Carbon	48.05
Hydrogen	7.67
Nitrogen	0.70
Oxygen*	43.57
H/C atomic ratio	2.23
O/C atomic ratio	0.13
HHV (MJ/kg)	20.46

*Calculated by difference

Table 2 Physicochemical properties of the HZSM-5 zeolite and dolomite catalysts

Catalyst	BET surface area (m^2/g)	Micropore volume (cm^3/g)	dp (Å)	Acidity (mmol NH_3/g cat.)
HZSM-5 zeolite	377	0.098	5.2–5.5	0.765
Dolomite	23	0.0026	173	-----

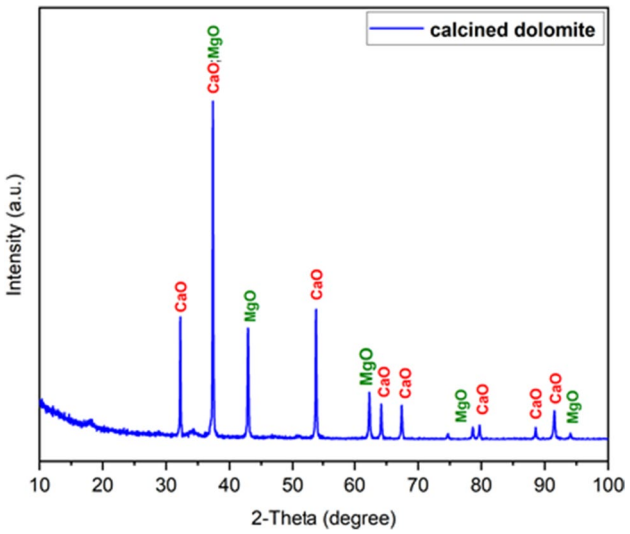

Fig. 1 The XRD diagram of the calcined dolomite

the dolomite is a basic one. The HZSM-5 has a silica/alumina ratio of 30, which confers high total acidity upon this catalyst.

The main mineral constituents of the calcined dolomite used have been determined by X-ray fluorescence (XRF) analysis. The chemical composition is as follows: MgO (wt. %) 43.61, SiO_2 (wt. %) 0.12, Fe_2O_3 (wt. %) 0.02, CaO (wt. %) 56.07, Al_2O_3 (wt. %) 0.15, Na_2O (wt. %) 0.01, and TiO_2 (wt. %) 0.02.

Fig. 1 shows the XRD diagram of the calcined dolomite.

As observed, all the peaks correspond to MgO and CaO phases.

Both analyses show that the main components of the dolomite catalyst are CaO and MgO, which are oxides containing basic sites. Besides, its specific surface area (BET area) is very low and therefore has a small number of strong acid sites available. In addition, it has a slightly developed surface structure leading to low activity. Nevertheless, the HZSM-5 zeolite has a high specific surface area and strong acidity, leading to a great number of surface acid sites on its surface. Accordingly, the better properties of the HZSM-5 zeolite are responsible for its higher cracking capacity, as well as higher deoxygenation capacity.

3.3 Py-GC/MS results

In this section, the results obtained in the catalytic pyrolysis on the HZSM-5 zeolite and dolomite catalysts are shown and they are compared with those obtained in a previous study carried out without any catalyst [33].

3.3.1 Thermal pyrolysis

In order to determine the effect of the catalysts on the volatile product distribution, the results obtained without catalyst are firstly shown in this subsection.

The volatiles generated in the pyrolysis of biomass cover a wide range of compounds of different nature, which may be classified as acids, ketones, aldehydes, phenols, alcohols, furans, ethers, and anhydrosugars, as well as hydrocarbons, N compounds, and S compounds in a much lower amount. Those preferred for biofuel are aromatic hydrocarbons, aliphatic hydrocarbons, and alcohols, whereas phenols and furans are regarded as high added-value chemicals. Acids are responsible for the corrosiveness of the bio-oil, and they are therefore undesired compounds. The same stands for ketones and aldehydes, which are related to the instability of the bio-oil during transport and storage. Ethers, esters, and oxygenates in general are also undesired compounds, as they reduce the heating value of the bio-oil. Polyaromatic hydrocarbons and nitrogen and sulfur compounds are detrimental for the environment [12].

Figure 2 shows the total ion chromatogram corresponding to the fast pyrolysis of DPS performed at 450 °C

Table 3 shows the retention times, compound names, and peak area percentages of the main compounds obtained in the thermal pyrolysis at 450 °C.

As observed, ketones (acetone and 1-hydroxy-2-propanone), acids (acetic, undecanoic, dodecanoic, and octadecanoic), and anhydrosugars (levoglucosan) are the prevailing compound families. In addition, the content of 5-(hydroxymethyl)-2-furancarboxaldehyde is also considerable.

Table 4 shows the peak area percentages of the different compound families obtained by the chromatographic analysis of the outlet stream of the pyrolysis of DPS samples at 450 and 500 °C.

As observed, anhydrosugars, acids, ketones, and furans are the more abundant compound families in the condensable fraction obtained. The content of acids and furans increases moderately with temperature, whereas that of anhydrosugars decreases. The sugar content decreases (from 23.1% at 450 °C to 19.2% at 500 °C). Levoglucosan is the most abundant compound in the sugar family.

In the acid product-fraction, acetic acid, long-chain acids (fatty acids), and alkyl ester acids are the prevailing ones. The main individual compounds identified are

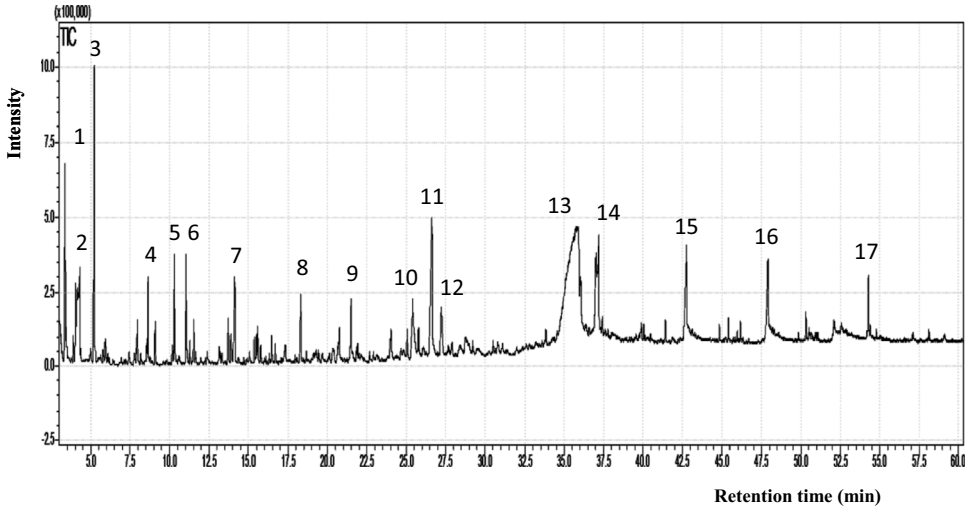

Fig. 2 Chromatogram obtained in the pyrolysis of the DPS sample, *T*=450 °C

Table 3 Retention times, compound names, and peak area percentages of the main compounds obtained in the thermal pyrolysis at 450 °C

Peak number	Retention time (min)	Compound	Peak area (%)
1	3.36	Acetone	2.51
2	4.31	Acetic acid	2.13
3	5.21	1-Hydroxy-2-propanone	3.27
4	8.64	Acetic anhydride	0.84
5	10.30	Furfural	1.51
6	11.05	2-Furanmethanol	1.30
7	14.14	Cyclohexanone	1.35
8	18.30	3-Methyl-1,2-cyclopentanedione	0.98
9	21.49	Cyclopropyl carbinol	0.86
10	25.41	1,4:3,2-Dianhydro-D-glucopyranose	2.07
11	26.63	5-(Hydroxymethyl)-2-furancarboxaldehyde	4.18
12	27.22	3,4-Anhydro-D-galactosan	1.28
13	35.87	Levoglucosan	20.89
14	37.20	Undecanoic acid	2.54
15	42.77	Dodecanoic acid	2.45
16	47.91	Octadecanoic acid	2.13
17	54.28	9-Octadecenal	0.70

acetic acid, decanoic acid, undecanoic acid, dodecanoic acid, and octadecanoic acid, with the concentration of each of them being of around 2% at 450 °C. Among the ketones, acetone prevails, with its concentration being in the 2.2–2.4% range. The remaining compounds in this ketones family (others) are mainly linear and cyclic C_3-C_8 ketones.

Among the furan family, 5-hydroxymethyl-2-furancarboxaldehyde was the main compound identified with high concentration, followed by furfural and furan derivatives. Its total concentration increased moderately from 9.6% at 450 °C to around 14% at 500 °C.

3.3.2 Catalytic pyrolysis on the HZSM-5 zeolite

As observed in the previous section, the oxygenated compounds are the predominant ones in the volatile stream obtained. This high oxygenated compound content confers undesirable properties, such as high acidity, instability, and low heating value, upon the bio-oil for liquid fuel applications, as well as great difficulty for valuable chemical extraction [36]. Therefore, upgrading of crude bio-oil is necessary to improve fuel properties or increase the concentration of valuable chemicals. The addition of catalysts in the pyrolysis process is a good option to overcome this problem. Thus,

Table 4 Mean peak area percentages (95% confidence interval) of the different compound families obtained in the thermal pyrolysis of DPS at 450 and 500 °C

	450 °C	500 °C
Incondensable gases	**16.4±0.3**	**12.2±0.4**
Acids	**16.9±2.6**	**20.2±2.0**
Acetic anhydride	0.7±0.2	0.6±0.2
Acetic acid	2.2±0.1	2.0±0.2
Formic acid	0.3±0.1	0.2±0.01
Fatty acids	11.5±2.5	12.1±4.0
Esters (alkyl ester acids)	2.3±0.3	5.3±2.4
Ketones	**15.7±0.5**	**16.4±2.3**
Acetone	2.4±0.1	2.2±1.0
1-Hydroxy-propanone	3.3±0.1	1.4±1.6
2,3-Butanedione	1.2±0.1	1.6±0.3
Cyclohexanone	1.3±0.1	0.7±1.0
Pyran derivatives	0.45±0.1	0.4±0.1
Others	7.0±0.3	10.1±0.1
Aldehydes	**2.7±0.1**	**2.7±0.1**
Phenols	**2.8±0.1**	**3.8±1.4**
1,2-Benzenediol	-	1.0±0.3
3-Methyl-1,2-benzenediol	0.8±0.4	0.6±0.3
Phenol	0.4±0.1	0.6±0.02
Phenol derivatives	1.4±0.2	1.4±0.7
Others	0.1±0.02	0.2±0.04
Ethers	**0.7±0.2**	**0.5±0.01**
Alcohols	**1.9±0.03**	**2.0±1.3**
Lineal	1.7±0.05	1.3±0.7
Cyclic	0.2±0.02	0.8±0.5
Furans	**9.6±0.9**	**14.4±0.5**
Furan derivatives	3.5±0.2	3.6±0.7
Furan derivatives (ketones)	0.7±0.1	0.7±0.04
Furan derivatives (aldehydes)	3.9±0.9	8.0±1.4
Furfural	1.5±0.04	2.0±0.3
Anhydrosugars	**23.1±4.7**	**19.2±1.0**
Levoglucosan	18.3±3.7	13.1±1.0
D-Allose	0.9±1.2	1.6±0.7
2,3-Anhydro-D-mannosan	0.4±0.1	0.5±0.1
3,4-Anhydro-D-galactosan	1.3±0.1	2.3±0.02
Dianhydro glucopyranose	2.2±0.2	1.8±0.6
HC	**0.3±0.1**	**0.3±0.1**
Aliphatics	0.01±0.01	0.1±0.1
Aromatics	0.3±0.1	0.1±0.2
N compounds	**0.3±0.02**	**0.3±0.1**
Pyrrole	0.2±0.03	0.3±0.1
S compounds	**0.6±0.1**	**0.4±0.01**
Methanethiol	0.6±0.1	0.2±0.3
Pyrans	**0.004±0.01**	**0.03±0.04**
Non-identified compounds	**9.1±3.7**	**7.3±5.5**

The bold entries significance is to remake the different families categories

catalysts with suitable properties favor deoxygenation reactions, and they therefore allow (i) obtaining bio-oils with low oxygen content for liquid fuel applications [37]; (ii) decreasing the content of the oxygenated compounds, and so reducing the acid content in the bio-oil; (iii) removing the unstable components, such as aldehydes and ketones; and (iv) increasing the content of phenols and hydrocarbons, especially those of monocyclic aromatic hydrocarbons (promising products for both liquid fuels and chemical raw materials). The last one not only improves the energy density of the bio-oil, but also makes it easier to blend it with crude oil [38].

Thus, Huynh et al. [39] used HZSM5, Zn/HZSM-5, and Fe/HZSM-5 catalysts for upgrading the pyrolysis oil. They observed that the quality of the oil was improved, as fuels with higher heating value and lower acidity and viscosity were obtained. They determined that the total combustion characteristic index of pyrolysis oils increased and that they were more flammable than fuel oil. These results prove that the upgraded oil might be used as fuel oil in industrial applications.

Concerning high-quality fuels, a high content of aliphatic hydrocarbons is essential, as well as the presence of aromatic hydrocarbons to improve the octane number of the fuel [40]. Besides, aliphatic and aromatic hydrocarbons increase the higher heating value of the bio-oil [41].

Product distribution at 450 °C Figure 3 shows the total ion chromatogram corresponding to the catalytic pyrolysis of DPS on the HZSM-5 zeolite (C/B=1, 2, 5) performed at 450 °C.

Table 5 shows the retention times, compound names, and peak area percentages of main compounds obtained in the catalytic pyrolysis on the HZSM-5 zeolite at 450 °C.

When a C/B=1 is used, the formation of aromatic compounds is remarkable, i.e., toluene, p-xylene, 1,2,3-trimethyl-benzene, and 2,3-dimethyl-naphthalene. The most abundant compounds correspond to ketones, acids, and anhydrosugars. For C/B=2, the increase in the relative content of aromatic compounds is worth mentioning, which is not the case when a C/B ratio of 5 is used. Furthermore, the relative content of acetaldehyde increases and those of acids and anhydrosugars decrease when the C/B ratio is raised.

Table 6 shows the peak area percentages of the different compound families obtained by the chromatographic analysis of the outlet stream in the catalytic pyrolysis of DPS samples at 450 °C on the HZSM-5 zeolite.

As observed in Table 6, the most abundant compound family is the one of incondensable gases. Its content increases significantly (from 23.6 to 54.1%) as catalyst/biomass (C/B) ratio is increased from 1 to 5. Only certain compounds have been identified in this lump, with propene being the most significant one, especially when the highest

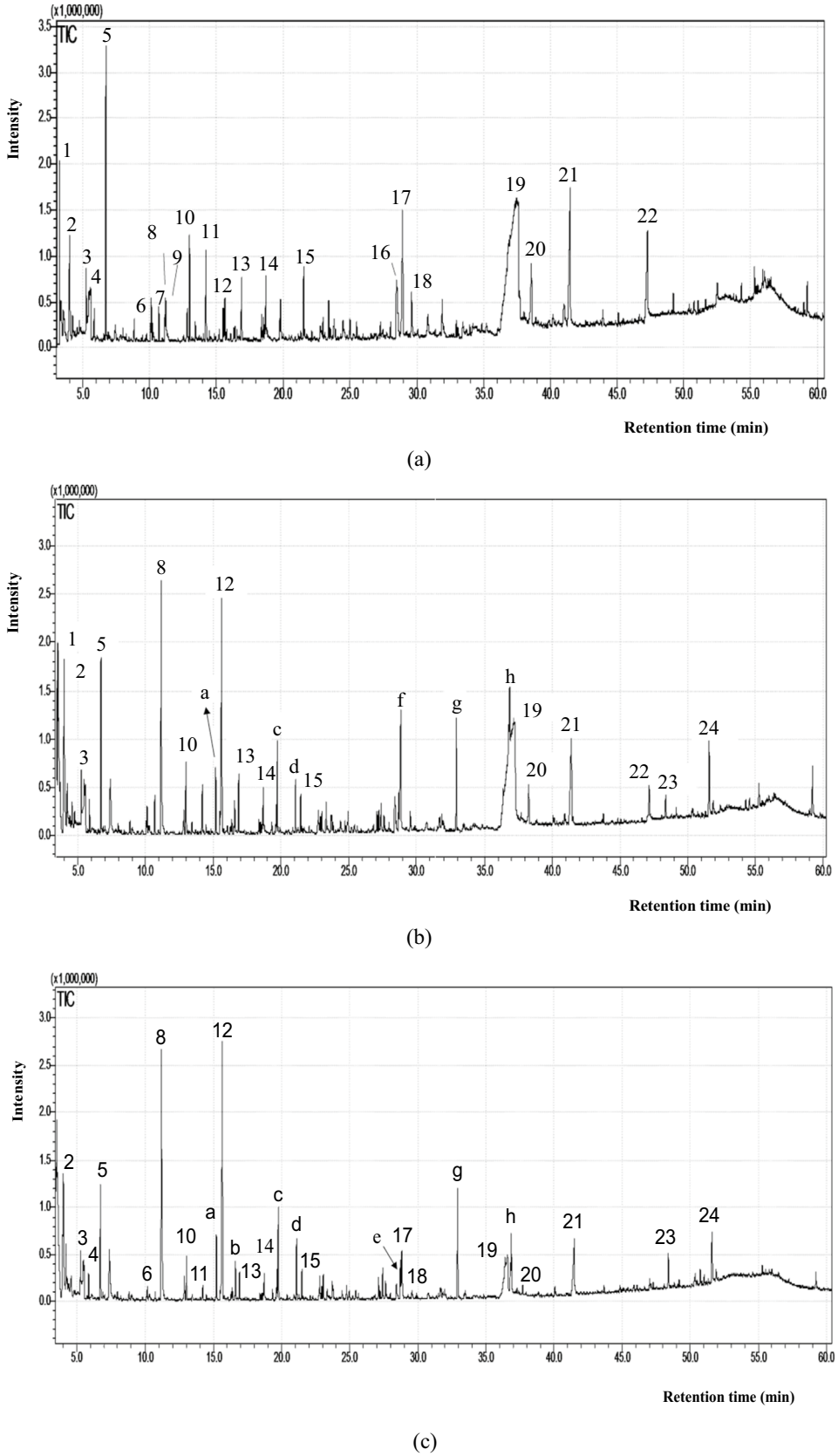

Fig. 3 Chromatogram obtained in the catalytic pyrolysis of DPS on the HZSM-5 zeolite at (**a**) C/B=1, (**b**) C/B=2, and (**c**) C/B=5, at *T*=450 °C

Table 5 Retention times, compound names, and peak area percentages of the main compounds obtained in the catalytic pyrolysis on the HZSM-5 zeolite (C/B=1, 2, 5) at 450 °C

Peak number	Retention time (min)	Compound	Peak area (%)		
			C/B=1	C/B=2	C/B=5
1	3.39	Acetaldehyde	0.76	1.17	3.14
2	4.0	Acetone	1.99	2.64	1.94
3	5.28	2,3-Butanedione	0.84	0.81	0.32
4	5.65	Acetic acid	0.83	0.6	0.04
5	6.74	1-Hydroxy-2-propanone	4.10	1.87	1.04
6	10.15	Acetic acid, propyl ester	0.65	-	0.12
7	10.72	Propanoic acid, 2-oxo, methyl ester	0.46	0.18	0.08
8	11.18	Toluene	0.70	3.18	3.73
9	11.25	Carbonocyanidic acid, ethyl ester	0.73	0.52	-
10	13.02	Furfural	1.59	0.84	0.46
11	14.25	1-Acetyloxy-2-propanone	1.73	0.23	0.12
a	15.21	Ethylbenzene	0.19	0.67	0.72
12	15.66	p-Xylene	0.73	1.84	2.72
b	16.6	m-Xylene	0.09	0.24	0.40
13	16.93	2-Methylcyclopentanone	1.09	0.54	0.30
14	18.73	5-Methyl-2-furancarboxaldehyde	0.96	0.61	0.31
c	19.76	1,2,3-Trimethyl-benzene	0.66	1.01	0.91
d	21.1	1,2,4-Trimethyl-benzene	0.10	0.61	0.67
15	21.53	3-Methyl-1,2-cyclopentanedione	1.30	0.60	0.32
16	28.46	1,2-Benzenediol	1.91	0.43	0.25
e	28.72	Naphthalene	0.07	0.46	0.79
f	28.83	1-Methyl-4-(1-methyl-2-propenyl)-benzene	-	1.93	-
17	28.92	5-(Hydroxymethyl)-2-furancarboxaldehyde	3.31	-	0.84
18	29.61	2,3-Anhydro-d-mannosan	1.11	0.33	0.12
g	32.93	1-Methyl-naphthalene	0.24	1.49	1.28
19	37.49	Levoglucosan	13.51	8.73	2.55
h	36.85	2,3-Dimethyl-naphthalene	0.61	0.79	0.70
20	38.59	D-Allose	1.86	0.88	0.15
21	41.51	Dodecanoic acid	6.05	7.91	1.53
22	47.28	Tetradecanoic acid	2.88	0.78	0.08
23	48.39	Anthracene	-	0.53	0.43
24	51.6	9-Methyl-anthracene	0.29	0.57	0.77

C/B ratio of 5 is used. This is a consequence of cracking, decarbonylation, and decarboxylation reactions promoted by the HZSM-5 zeolite due to its acidity (Si/Al=30).

The second most abundant compound family is the one of hydrocarbons. This lump accounts for aromatic and non-aromatic compounds. The content of non-aromatic compounds decreases slightly from 1.2 to 0.7% when the B/C ratio is increased, whereas that of aromatic compounds (prevailing fraction in this lump) increases markedly from 5.9% when the C/B ratio is 1 to 23.8% when the C/B is 5. Toluene, xylenes, naphthalene derivatives, and benzene derivatives are the most abundant compounds identified. Other compounds identified are indane, indene, fluorene, anthracene and their derivatives, and biphenyl.

Figure 4 shows the peak area evolution of the whole aromatic family, and of benzene, toluene, xylenes, and polyaromatic hydrocarbons (PAH), when different catalyst/biomass (C/B) mass ratios are used. As observed, the area increases when the C/B ratio is increased, and especially when C/B=5 is used. This is the consequence of the reactions favoring the formation of aromatic compounds, which are enhanced when a higher amount of zeolite is used.

Regarding the PAH fraction, the compounds identified are naphthalene, fluorene, anthracene, and their derivatives, with naphthalene and its derivatives being the most abundant ones.

This high concentration of hydrocarbon compounds is a consequence of the deoxygenation caused by the HZSM-5

Table 6 Mean peak area percentages (95% confidence interval) of the different compound families obtained in the catalytic pyrolysis of DPS at 450 °C when the C/B mass ratios of 1, 2, and 5 are used

	Biomass/catalyst (B/C) mass ratio		
	1/1	1/2	1/5
Incondensable gases	**23.6±5.5**	**32.5±2.3**	**54.1±4.1**
Propene	1.7±0.3	5.3±0.5	11.4±1.1
2-Methyl-1-propene	2.0±2.3	2.8±1.2	3.6±0.9
1-Butene	-	1.6±0.6	1.3±0.3
Acids	**11.7±2.3**	**11.4±3.3**	**2.4±0.2**
Acetic acid	1.1±0.2	1.0±0.5	0.2±0.2
Fatty acids	7.6±2.3	9.5±2.3	1.8±0.2
Esters (alkyl ester acids)	2.6±0.02	1.0±0.1	0.4±0.2
Ketones	**14.8±3.2**	**8.6±1.1**	**5.4±0.8**
Acetone	2.0±0.01	2.7±0.4	1.7±0.4
1-Hydroxy-propanone	3.6±0.7	1.9±0.3	0.8±0.3
2,3-Butanodione	0.9±0.1	0.7±0.01	0.3±0.04
2-Butanone	0.8±0.1	0.8±0.4	0.4±0.1
Others	7.5±2.6	2.9±0.5	2.3±0.02
Aldehydes	**1.5±0.5**	**1.7±0.2**	**3.2±0.4**
Acetaldehyde	0.6±0.2	1.1±0.1	2.9±0.3
Phenols	**3.3±1.2**	**1.2±0.5**	**0.7±0.04**
1,2-Benzenediol	1.5±0.6	0.5±0.2	0.2±0.07
1,2-Benzenediol derivatives	1.0±0.4	-	0.04±0.005
1,4-Benzenediol (hydroquinone)	-	0.2±0.01	0.06±0.08
1,4-Benzenediol derivatives	0.2±0.03	0.1±0.1	0.02±0.03
Phenol	0.1±0.02	-	0.01±0.01
Phenol derivatives	0.5±0.2	0.3±0.1	0.4±0.2
Ethers	**0.4±0.0**	**-**	**0.3±0.2**
Alcohols	**2.2±0.2**	**0.5±0.3**	**0.5±0.04**
Lineals	1.9±0.2	0.5±0.3	0.4±0.07
Cyclics	0.2±0.1	-	0.02±0.02
Furans	**7.4±1.4**	**3.6±0.8**	**1.9±1.3**
Furane	0.4±0.1	0.7±0.1	0.3±0.1
Furane derivatives	1.2±0.1	0.8±0.1	0.4±0.2
Furane derivatives (ketones)	0.7±0.2	0.4±0.05	0.2±0.2
Furane derivatives (aldehydes)	3.7±0.8	0.7±0.2	0.7±0.6
Furfural	1.4±0.3	1.0±0.3	0.3±0.2
Anhydrosugars	**18.0±1.9**	**8.7±7.1**	**2.5±0.6**
Levoglucosane	15.1±2.3	7.8±6.7	2.2±0.5
D-Allose	1.9±0.004	0.5±0.4	0.2±0.03
2,3-Anhydro-D-mannosan	0.9±0.3	0.4±0.1	0.1±0.04
2,3-Anhydro-D-galactosan	-	-	0.03±0.04
Dianhydro glucopyranose	0.2±0.1	0.1±0.03	0.06±0.002
Hydrocarbons	**7.1±1.1**	**19.9±0.3**	**24.5±6.1**
Aliphatics	1.2±0.5	1.5±0.4	0.7±0.3
Aromatics	5.9±0.6	18.3±0.7	23.8±6.4
N compounds	**1.9±0.7**	**1.3±0.01**	**0.6±0.5**
Acetonitrile	0.3±0.2	0.8±0.002	0.3±0.3
S compounds	**0.1±0.2**	**2.1±0.01**	**2.0±0.1**
Methanethiol	0.1±0.2	2.1±0.01	2.0±0.1
Non-identified compounds	**8.1±0.2**	**8.2±1.0**	**1.7±1.6**

The bold entries significance is to remake the different families categories

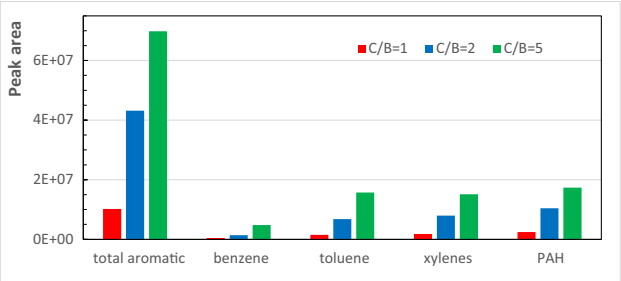

Fig. 4 Evolution of the total aromatic content and those of benzene, toluene, and xylenes for different catalyst/biomass ratios

zeolite. Many authors have determined that HZSM-5 zeolites change the composition of the bio-oils by both reducing the amount of oxygenate compounds via deoxygenation reactions and increasing the aromatic species, which leads to an organic fraction (bio-oil) that can be upgraded to gasoline and diesel fuels [10, 42, 43].

Carlson et al. [44] determined that the first stage in cellulose degradation involves dehydration reactions to form anhydrosugars, and they subsequently undergo acid-catalyzed dehydration on the active sites of the catalyst, leading to the formation of dehydrated products. These products undergo further oligomerization, decarboxylation, and decarbonylation, or cracking reactions, to form C_2-C_6 olefins, which then combine to yield aromatics. The deoxygenation leads to the production of CO, CO_2, and H_2O.

Figure 5 shows the evolution of the content of C_3-C_7 olefins in the catalytic pyrolysis carried out at 450 °C when the C/B ratios of 1, 2, and 5 are used. As observed, the content of the lighter C_3-C_4 olefins (propene, 2-methyl-propene, 2-butene) increases markedly as the C/B ratio is increased, whereas that of C_5-C_7 ones (2-pentene, 2-methyl-1-butene, 3-hexene, 3-methyl-1,3,5-hexatriene) goes through a slight

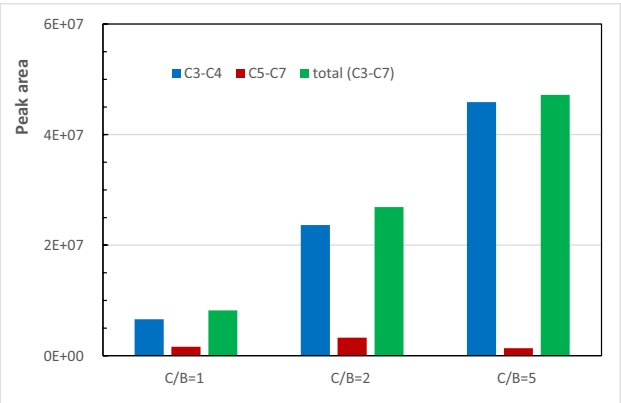

Fig. 5 Distribution of C_3-C_7 olefins in the catalytic pyrolysis at 450 °C for different catalyst/biomass ratios

peak for the C/B of 2. These results are evidence that the HZSM-5 zeolite favors the reactions leading to olefin formation. The increase in light olefin content by an increase in the catalyst amount was also observed by Shahsavari and Sadrameli [45] in their study of biomass catalytic pyrolysis on Sn and Re doped HZSM-5 zeolite catalysts in a fixed bed tubular reactor. They obtained lower ethene and propene yields when the catalyst amount was lower due to the reduction in the dehydrogenation rate of paraffins and their conversion into olefins. Adjaye and Bakhshi [46] proposed that the light oxygenated organic compounds are converted into olefins, and they then go on to aromatize.

Anhydrosugar prevails for the C/B ratio of 1 (18.0%), but their content decreases markedly when the C/B ratio is increased to 2 and 5 (8.7% and 2.5%, respectively) (Table 6). The prevailing compound in this family is levoglucosan, and its relative content decreases as the C/B ratio is increased, from 13.1% for the C/B ratio of 1 to 2.2% for the C/B ratio of 5. It should be noted that levoglucosan is the main degradation compound of cellulose. The decrease in its concentration by increasing the C/B ratio may be explained by the cracking reactions promoted by the HZSM-5 zeolite [47, 48].

Mihalcik et al. [10] reported that deoxygenation of levoglucosan is another reaction leading to aromatic compound formation, following 2 steps, as are (i) dehydration to form furans and similar compounds and (ii) conversion of the furans into aromatics via further dehydration and decarboxylation. Foster et al. [49] also reported that anhydrosugars are aromatic compound precursors in the glucose catalytic pyrolysis carried out in a semi-batch Pyroprobe. They determined that the anhydrosugars stem from glucose dehydration reactions and undergo further dehydration to form furan compounds and water. These furans follow a route involving the formation of a carbocation hydrocarbon pool and carbon monoxide by decarbonylation and oligomerization reactions on the zeolite. This hydrocarbon pool is then transformed into non-oxygenated olefins, as well as single-ring and polycyclic aromatic compounds. Liu et al. [50] also reported that the partial cracking of β-1,4-glycosidic bonds in the cellulose generates BTX and phenol through the reactions of dehydration, decarbonylation, decarboxylation, and oligomerization. Lazaridis et al. [51] established that phenolic compounds are converted into aromatics by oligomerization, as well as cracking and dehydration, on zeolite catalysts. Deoxygenation of ketones is another route leading to the formation of aromatic compounds. Adjaye and Bakhshi [52] established that this process takes place through decarbonylation.

Table 6 shows that the ketones family is also an abundant one, as its relative content ranges from around 15 to 5% for C/B ratios ranging from 1 to 5. Acetone is the most significant compound identified, with its content ranging from 2.7 to 1.7% for C/B ratios from 1 to 5. Other compounds identified are ketones with 5 to 7 carbon atoms, and aliphatic and cyclic compounds, whose relative content decreases as the C/B ratio is increased. Concerning the acid family, its content also decreases by increasing the C/B ratio, from 11.7% for the C/B ratio of 1 to 2.4% for the C/B ratio of 5. The main N compounds identified have been acetonitrile, indole, dodecanenitrile, pentadecanenitrile, and nonadecanenitrile. Methanethiol has been the only sulfur compound identified. These compounds are derived from the nitrogen and sulfur the date palm seed contains.

Effect of the HZSM-5 catalyst at 450 °C Figure 6 shows the percentages of the peak areas obtained for the components in the pyrolysis stream without catalyst and with different amounts of HZSM-5 zeolite catalysts at 450 °C. Thermal pyrolysis of DPS was conducted in a previous study in the same reactor [33].

As observed, the lump of incondensable gases is the most abundant one, with a relative content increasing greatly in the catalytic pyrolysis (from C/B=2 to 5). This is a consequence of the cracking reactions favored by the HZSM-5 zeolite, which lead to a high concentration of incondensable gases. Mihalcik et al. [10] conducted pyrolysis in an Auto-Shot Sample at 550 °C on different zeolites and determined a significant increase in the non-condensable gases with respect to the non-catalytic pyrolysis (from 15 wt.% in the thermal pyrolysis to 30.9 wt.% on the HZSM-5 zeolite catalyst (Si/Al=23) at the mass ratio of B/C=1/5).

The relative content of anhydrosugars decreases in the presence of the catalyst, with the lowering being more pronounced as the catalyst quantity is higher. The most abundant compound identified is levoglucosan. The acid family decreases also markedly in the presence of the catalyst. This decrease is the result of the reduction in the concentration of long-chain acids, such as decanoic, dodecanoic, and octadecanoic acids. Furthermore, the concentration of acetic acid is insignificant in the presence of the zeolite. Jeon et al. [53] reported that a microporous zeolite like the HZSM-5 reduces the acid yield due to their decomposition to give smaller molecules.

The concentration of ketones and furans also decreases in the presence of the catalyst, especially at the C/B ratios of 2 and 5. In the case of ketones, all the compounds undergo reduction (acetone, 1-hydroxy-2-propanone, 2,3-butanedione, 2-butanone, and so on). In the case of furans, the decrease is due to the reduction in furane derivatives, i.e., aldehyde type furane derivatives, ketone type furane derivatives, and furfural. Cheng and Huber [54] and Nikbin et al. [55] reported that furanic compounds react with olefins to form intermediate compounds, which by means of dehydration produce toluene and p-xylene. This may explain the

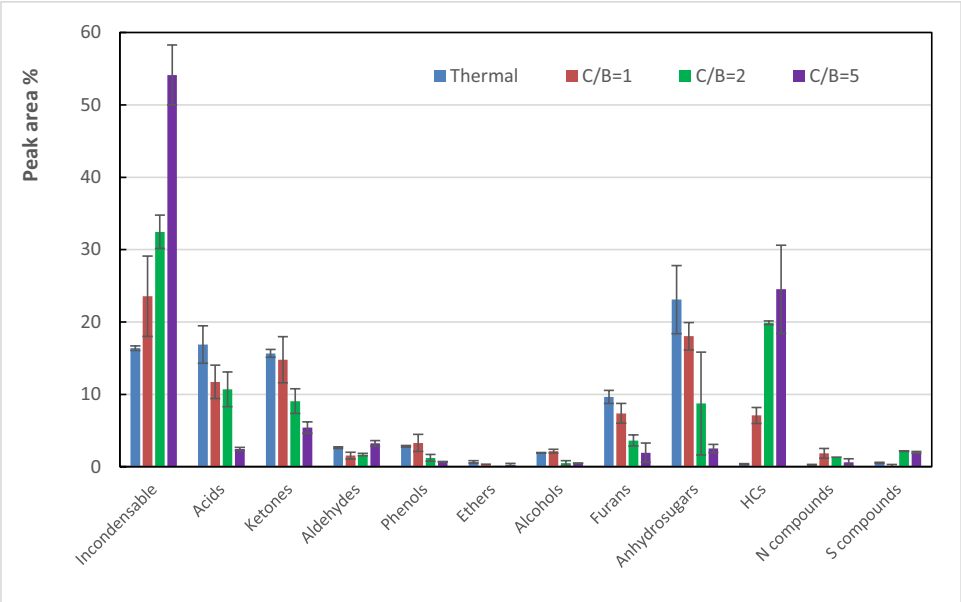

Fig. 6 Peak area percentages of the products obtained in the thermal pyrolysis and catalytic pyrolysis of DPS with different biomass/catalyst mass ratios at 450 °C

reduction observed in furans in the presence of the HZSM-5 zeolite.

Another remarkable difference is the great increase observed in the content of hydrocarbons (from 0.35% in the thermal pyrolysis to around 25% in the catalytic one at C/B=5). This result is a consequence of the deoxygenation promoted by the HZSM-5 zeolite. As observed in Fig. 5, the yield of aromatic compounds is higher as the C/B ratio is higher. Benzene derivatives, toluene, xylenes, and naphthalene derivatives are the prevailing compounds identified.

This effect was also observed by Vichaphund et al. [56], but at a higher temperature (500 °C). They observed a marked effect of the B/C ratio on the formation of aromatic compounds when they carried out biomass pyrolysis on a HZSM-5 catalyst with C/B ratios in the 1 to 10 range in a Pyroprobe. Thus, they reported the highest yield of aromatic compounds for the highest C/B ratio.

Another significant difference between thermal and catalytic pyrolysis is the formation of nitriles, with acetonitrile being the most abundant one with a relative content of 0.8% at C/B=2, followed by dodecanenitrile, pentadecanenitrile, and nonadecanenitrile, with values in the 0.1–0.2% range. In the thermal pyrolysis, pyrrole and pyridine were the sole compounds identified, with their contents being of around 0.24% and 0.06%, respectively. Anand et al. [57] conducted catalytic pyrolysis of algae on zeolites and reported that the main species of nitrogen-containing compounds were nitriles. They attributed their formation at high temperatures to the dehydration of amides. Setter et al. [58] also found an increase in nitriles in the catalytic pyrolysis oil, probably due to the increased rate of decomposition of proteins and carbohydrates due to their transformation by deamination reactions.

Overall, the use of the HZSM-5 zeolite involves beneficial effects, since its activity reduces markedly the concentration of oxygenated compounds, such as acids, ketones, furans, and anhydrosugars. Acids are responsible for the acidity of the bio-oil fraction, which causes corrosiveness. Furthermore, ketones are related to the instability of the bio-oil fraction during transport and storage. This reduction of oxygenated compounds leads to a dramatic increase in the content of aromatic hydrocarbons.

Product distribution at 500 °C Table 7 shows the mean peak area percentages of the compound families identified in the catalytic pyrolysis of DPS at 500 °C using a C/B mass ratio of 1. As observed, the relative content of acids, anhydrosugars, and ketones is high, as well as those of hydrocarbons and incondensable gases, as they are promoted by the joint effect of both the zeolite catalyst and the temperature.

Influence of temperature on the catalytic pyrolysis on the HZSM-5 catalyst Figure 7 shows the peak area percentages obtained at 450 and 500 °C with a C/B mass ratio of 1 in both thermal pyrolysis and catalytic pyrolysis on the HZSM-5. As observed, the content of incondensable gases is high, especially for the higher temperature of 500 °C. The content of acids is slightly higher at 500 °C due to the increase in the long-chain acids, such as octanoic, dodecanoic, tetradecanoic, and octadecanoic ones. The relative content of hydrocarbons at 500 °C is double that at 450 °C, with both linear and aromatic compounds being responsible for this trend.

Figure 8 shows the peak areas of the aromatic compounds at both temperatures. As observed, temperature plays a crucial role in the increase of aromatic compounds in the catalytic pyrolysis on the HZSM-5.

Table 7 Mean peak area percentages (95% confidence interval) of the different compound families obtained in the catalytic pyrolysis of DPS at 500 °C with the C/B mass ratio of 1

Incondensable gases	**27.7±3.2**
Propene	2.1±0.3
2-methyl-1-propene	3.2±0.4
1-butene	0.6±0.1
Acids	**13.1±0.03**
Acetic acid	0.9±0.1
Fatty acids	9.6±0.2
Esters (alkyl esters acids)	2.3±0.02
Ketones	**11.8±0.004**
Acetone	2.4±0.2
1-hydroxy-propanone	2.1±0.1
2,3-butanedione	0.8±0.15
2-butanone	5.7±0.5
Others	0.7±0.4
Aldehydes	**1.2±0.1**
Acetaldehyde	0.7±0.1
Phenols	**2.1±0.15**
1,2-benzenediol	0.8±0.1
1,2-benzenediol derivatives	0.2±0.03
1,4-benzenediol (hydroquinone)	0.3±0.05
1,4-benzenediol derivatives	0.3±0.01
Phenol	0.1±0.004
Phenol derivatives	0.5±0.05
Ethers	**0.3±0.06**
Alcohols	**1.6±0.2**
Lineal	1.3±0.2
Cyclic	0.3±0.001
Furans	**7.4±0.9**
Furan	0.7±0.035
Furan derivatives	1.6±0.3
Furan derivatives (ketones)	0.9±0.1
Furan derivatives (aldehydes)	3.0±0.4
Furfural	1.1±0.06
Anhydrosugars	**14.0±0.5**
Levoglucosan	12.9±0.35
D-allose	0.6±0.2
2,3-anhydro-d-mannosan	0.3±0.02
Dianhydro glucopyranose	0.1±0.003
Others	0.1±0.0015
Hydrocarbons	**15.3±3.8**
Aliphatics	2.2±0.5
Aromatics	13.1±3.3
N compounds	**1.9±0.3**
Acetonitrile	1.0±0.2
S compounds	**1.6±0.15**
Methanethiol	1.6±0.15
Non identified compounds	**2.0±0.96**

The bold entries significance is to remake the different families categories

In general, the formation of aromatic hydrocarbons starts with the donation of a proton to substrates, such as hydrocarbons, on the acid sites of the catalyst. This protonation leads to the formation of a carbocation within the hydrocarbon, which gives olefins by β-hydrogen elimination reaction. These olefins are transformed into aromatics through oligomerization, cyclization, and hydrogen transfer reactions performed on the catalyst acid sites [59, 60].

The high content of BTX compounds determined is a consequence of the shape selectivity of the HZSM-5 zeolite, which has an average pore width in the 0.52–0.55 nm range. This pore size is suitable for the formation and diffusion of compounds like BTX within the pore system. Foster et al. [49] used a semi-batch Pyroprobe with microporous and mesoporous HZSM-5 catalysts and concluded that pure microporous HZSM-5 catalysts favor the production of small monoaromatic compounds (benzene, toluene, and xylene) in the pyrolysis of glucose and maple wood at a final reaction temperature of 600 °C.

According to these authors, micropore size is not the only factor to be considered, but internal pore spaces and steric hindrance play also a determining role in the formation of aromatics. They concluded that medium-pore zeolites with moderate internal pore spaces and steric hindrance (ZSM-5) contribute to increasing the aromatic yield and decreasing coke formation.

Another feature that affects the formation of aromatic compounds is acidity, which is related to the silica/alumina ratio. Foster et al. [49] also studied the effect of this parameter. They used silica/alumina ratio values of 23, 30, 50, and 80 and concluded that the maximum aromatic yield was obtained for SiO_2/Al_2O_3=30. A silica/alumina ratio of 30 leads to the highest availability of Brønsted sites. As the silica/alumina ratio is decreased, the concentration of acid sites increases. This increment in acid sites may favor secondary reactions leading to coke formation within the micropores by promoting the conversion of aromatic compounds.

Kim et al. [61] conducted the catalytic upgrading of the volatile stream generated in the pyrolysis (500 °C) of 2 biomasses and determined that their HZSM-5 zeolite with a silica/alumina ratio of 23 led to the highest BTX formation due to its high acidity and suitable pore size. They also studied the effect of the acid site concentration in the catalyst on the aromatic formation and reported that a HZSM-5 with a silica/alumina ratio of 23 produced a larger amount of aromatic compounds than a HZSM-5 with a silica/alumina ratio of 50, which is explained by the higher number of acid sites in the former.

Effect of the HZSM-5 catalyst at 500 °C Figure 9 shows the mean peak area percentages obtained in the thermal pyrolysis and catalytic pyrolysis on the HZSM-5 with a C/B ratio of 1 at 500 °C. As observed, there is a significant increase in

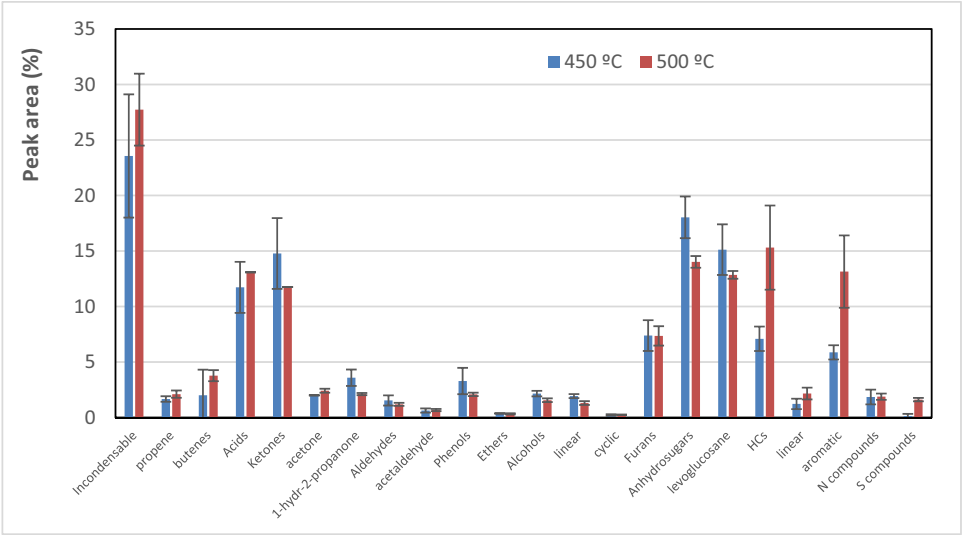

Fig. 7 Peak area percentages obtained at 450 and 500 °C with a C/B mass ratio of 1

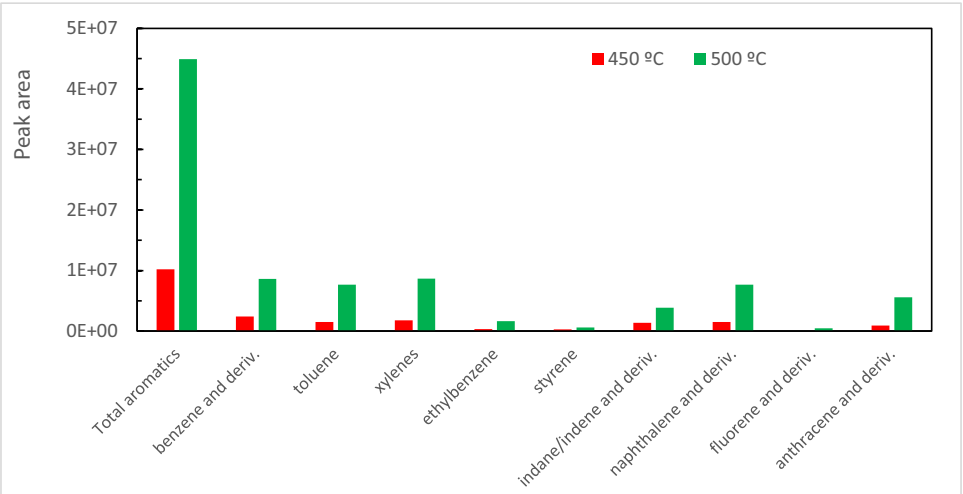

Fig. 8 Peak area of the total content of aromatic compounds and those of individual compounds for the catalytic pyrolysis on HZSM-5 at 450 and 500 °C

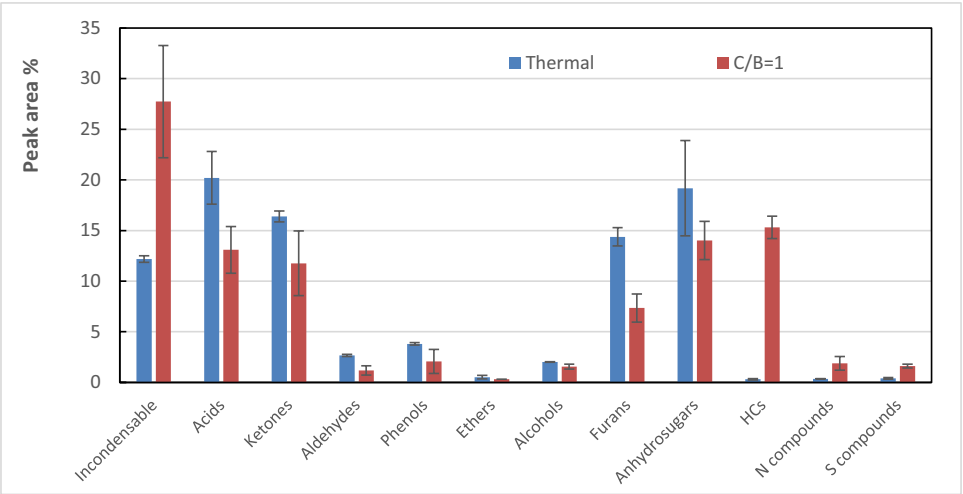

Fig. 9 Mean peak area percentages obtained in the thermal pyrolysis and catalytic pyrolysis with C/B ratio of 1 at 500 °C

the content of incondensable gases in the catalytic pyrolysis due to the cracking reactions promoted by the HZSM-5 zeolite. Vichaphund et al. [56] pyrolyzed biomass on a HZSM-5 catalyst in a Pyroprobe at 500 °C and determined that the presence of HZSM-5 catalyst increased the gas formation. They reported that large amounts of catalyst led to severe secondary cracking and decomposition reactions of the liquid product, resulting in higher gas yields under those conditions.

The hydrocarbon family also shows a dramatic increase in the catalytic pyrolysis, which is explained by the increase in the content of aromatic compounds favored by the HZSM-5 zeolite due to its deoxygenating effect. Nevertheless, acids, ketones, aldehydes, phenols, alcohols, furans, and sugars are hindered in the catalytic pyrolysis. Iliopoulou et al. [12] also observed a reduction in the yields of acids and ketones in the volatiles obtained in the pyrolysis carried out in a fixed bed tubular reactor at 500 °C on a HZSM-5 zeolite and modified zeolites.

Nguyen et al. [62] performed biomass catalytic pyrolysis on a faujasite catalyst in a fixed bed reactor at 500 °C and they observed a moderate reduction in the content of acids, a very pronounced one in those of aldehydes and ketones, and an increase in those of phenols and hydrocarbons in the bio-oil obtained. These trends involve a reduction in the acidity and instability, as aldehydes and ketones are responsible for condensation reactions causing viscosity increase. Furthermore, the increase in phenols and hydrocarbons improves the energy density of the bio-oil and also makes it easier to blend it with certain fractions of fossil crude oil [38].

Stephanidis et al. [63] approached the degradation of lignocellulosic biomass on different types of catalysts at 500 °C in a bench-scale unit equipped with a fixed bed. According to their studies, a strongly acid HZSM-5 zeolite promotes oxygen content reduction in the organic fraction, thereby decreasing the concentration of acids, ketones, and phenols in the biomass pyrolysis oil. These trends are evidence of the cracking and deoxygenating effect of the HZSM-5 zeolite, which contribute to increasing the formation of incondensable gases and aromatic hydrocarbons. Thus, according to Carlson et al. [44], zeolite catalysts selectively deoxygenate the pyrolytic vapors, leading to the formation of aromatic compounds.

Zhang et al. [64] also concluded that ZSM-5 catalysts give the highest yields of aromatics and olefins, when they treated straw biomass in a fluidized bed reactor at 550 °C on different types of catalysts.

Deoxygenating activity of the HZSM-5 catalyst As mentioned above, the deoxygenating capacity of the HZSM-5 zeolite is a well-known fact. The content of oxygenate compounds is an index of this capacity and the results corresponding to DPS samples are shown in Table 8, in which the mean peak area percentages of oxygenated compounds are displayed for thermal pyrolysis at 450 and 500 °C and catalytic pyrolysis at 450 °C.

As observed, the HZSM-5 zeolite reduces the content of oxygenated compounds, with both temperature and C/B ratio having a great influence. Thus, thermal pyrolysis at 450 °C leads to 98% oxygenates, whereas catalytic pyrolysis at this temperature decreases this content to 26% for a C/B ratio of 5. Concerning the effect of temperature, thermal pyrolysis at 500 °C allows obtaining an almost fully oxygenated stream (99% oxygenates), whereas catalytic pyrolysis at this temperature with a C/B ratio of 1 provides a stream with 70% oxygenates. A comparison of this value with the one obtained for the same C/B ratio at 450 °C shows that catalytic pyrolysis at a higher temperature lowers considerably the content of oxygenates, from 83 to 70%. This is explained by the enhancement of deoxygenation reactions as temperature is increased.

3.3.3 Catalytic pyrolysis on the dolomite catalyst

Figure 10 shows the total ion chromatogram corresponding to the catalytic pyrolysis of DPS on the dolomite catalyst (C/B=1) at 450 °C.

Table 9 shows the retention times, compound names, and peak area percentages of the most abundant compounds obtained in catalytic pyrolysis on the dolomite catalyst at 450 °C. As observed, long carbon chain ketones prevail (undecanone, tridecanone, heptadecanone, nonadecanone). Although levoglucosan is the more outstanding compound identified, others within the acid family are also abundant. Furthermore, contrary to what happened when the HZSM-5 zeolite was used, aromatic compounds are not

Table 8 Mean peak area percentages of oxygenated compounds in the thermal pyrolysis at 450 and 500 °C and catalytic pyrolysis of DPS at 450 °C

	Thermal 450 °C	Catalytic C/B=1	Catalytic C/B=2	Catalytic C/B=5	Thermal 500 °C	Catalytic C/B=1
Oxygenates	98±0.3	83±6.1	48±3.8	26±8.9	99±0.5	70±3.0

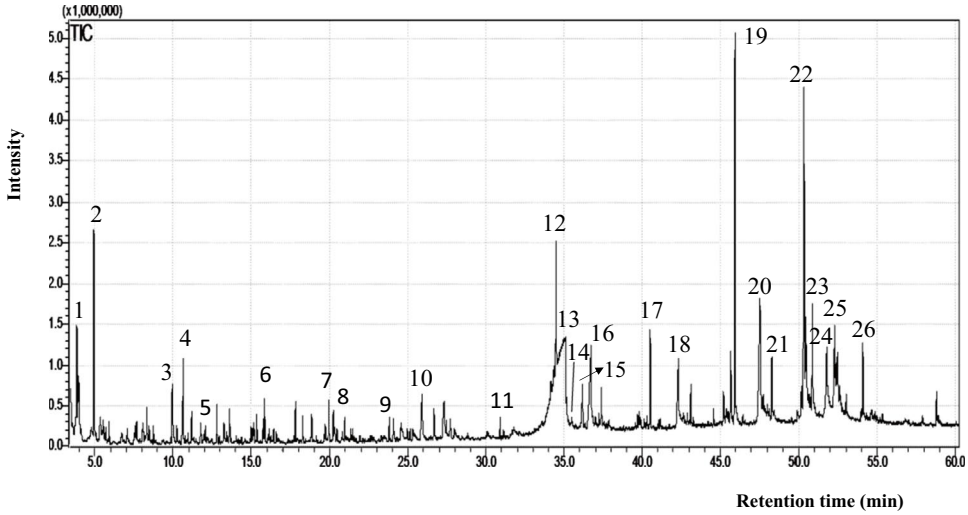

Fig. 10 Chromatogram obtained in the catalytic pyrolysis of DPS on the dolomite catalyst (C/B=1) at *T*=450 °C

Table 9 Retention times, compound names, and peak area percentages of the most abundant compounds obtained in the catalytic pyrolysis on the dolomite catalyst at 450 °C

Peak number	Retention time (min)	Compound	Peak area (%)
1	3.83	2,3-Butanedione	1.42
2	4.94	1-Hydroxy-2-propanone	2.05
3	9.95	2-Cyclopenten-1-one	0.44
4	10.65	Propanoic acid, 2-methyl, 2-propenyl ester	0.88
5	11.76	1-Nonene	0.30
6	15.85	1-Decene	0.45
7	19.9	3-Undecene	0.38
8	20.2	Undecane	0.37
9	23.79	1-Dodecene	0.23
10	25.91	5-(Hydroxymethyl)-2-furancarboxaldehyde	1.18
11	30.9	4-Tetradecene	0.21
12	34.50	2-Undecanone	1.24
13	34.50	Levoglucosan	17.66
14	35.17	D-allose	0.37
15	36.17	1,6-Anhydro-.beta.-talopyranose	0.70
16	36.71	Undecanoic acid	0.37
17	40.51	2-Tridecanone	1.03
18	42.32	Dodecanoic acid	1.43
19	45.96	2-Heptadecanone	4.66
20	47.55	Tetradecanoic acid	2.94
21	48.31	3-Octadecanone	0.72
22	50.33	1-Methoxy-9-octadecene	4.36
23	50.86	2-Nonadecanone	1.07
24	51.77	9-Octadecenoic acid	1.29
25	52.28	Octadecanoic acid	0.97
26	54.1	9-Octadecenal	0.74

the main ones. In this case, aliphatic compounds (linear hydrocarbons containing 5 to 18 carbon atoms) prevail.

Table 10 shows the peak are percentages of the compound families identified in the catalytic pyrolysis of DPS at 450 °C using a C/B mass ratio of 1. As observed, the ketones family is the most abundant one (26.9 peak area percentage), which contains long-chain compounds, such as undecanone, tridecanone, nonadecanone (approximately 1%), and 2-heptadecanone (approximately 5%). The high relative content of ketones is explained by the role played

Table 10 Peak area percentages of the different compound families obtained in the catalytic pyrolysis of DPS on dolomite at 450 °C with a C/B mass ratio of 1

	Peak area %
Incondensable gases	**13.2±3.7**
Acids	**16.5±3.9**
Acetic acid	0.2±0.06
Fatty acids	12.9±3.7
Esters (alkyl ester acids)	3.4±0.4
Ketones	**26.9±2.3**
Acetone	2.7±0.8
1-Hydroxy-propanone	2.3±0.25
2,3-Butanedione	1.5±0.1
2-Butanone	1.3±0.6
Others	19.0±1.5
Aldehydes	**2.7±0.5**
Acetaldehyde	1.3±0.4
Phenols	**2.4±0.5**
1,2-Benzenediol	0.6±0.3
1,2-Benzenediol derivatives	0.1±0.08
Phenol	0.3±0.03
Phenol derivatives	1.4±0.25
Ethers	**5.4±1.0**
Esters	**0.8±0.1**
Alcohols	**1.7±0.1**
Lineal	1.7±0.1
Cyclic	0.08±0.01
Furan	**3.2±1.2**
Furan derivatives	0.3±0.03
Furan derivatives (ketones)	0.4±0.1
Furan derivatives (aldehydes)	2.3±1.1
Furfural	0.09±0.04
Anhydrosugars	**16.6±5.8**
Levoglucosan	14.8±5.4
D-allose	0.25±0.2
2,3-Anhydro-D-mannosan	0.2±0.05
3,4-Anhydro-D-galactosan	0.6±0.15
Glucopyranose	0.1±0.02
Others	0.6±0.5
HC	**4.8±0.4**
Aliphatics	4.5±0.4
Aromatics	0.25±0.03
N compounds	**0.8±0.2**
S compounds	**0.7±0.2**
Methanethiol	0.7±0.2
Pyrans	**0.08±0.01**
Non-identified compounds	**4.5±2.2**

The bold entries significance is to remake the different families categories

by CaO as reactant; that is, the reaction of CaO with acids or other carboxyl groups yields calcium carboxylates, which are subsequently decomposed into $CaCO_3$ and ketones [65, 66]. Consequently, the relative content of acids decreases. This can also explain the high acetone, 2,3-butanedione, and 2-butanone peak areas obtained.

Other compounds identified in high percentages are 2-cyclopenten-1-one and derivatives, cyclopentanone and derivatives, 1-(acetyloxy)-2-propanone, and 2,3-pentanedione. Zhou et al. [67] reported that the significant formation of cyclic ketones can be explained by the transformation of anhydrosugars (mainly levoglucosan) via rearrangement reactions of furfuryl type compounds, such as furfural. Other authors explained this phenomenon as ketonization of carbolic acids to form acetone, which can couple with furans or acetone itself via aldol condensation to elongate the carbon chain length by numerous base catalysts [68, 69]. The results obtained in this study show that ketones have a markedly higher relative content and furans a significant decrease with respect to the values obtained in the thermal pyrolysis. Besides, the content of acids is lower, especially of short carbon chained ones, such as formic and acetic acids.

Valle et al. [23] upgraded the bio-oil on dolomite and obtained a high amount of acetone. They state that this result is evidence of the dolomite activity for acetic acid ketonization and, furthermore, other ketonization reactions involving carboxylic acids may also occur, which lead to the formation of linear ketones.

Anhydrosugar compounds are the next most abundant ones, with their content being 16.6%. Levoglucosan is the prevailing compound in this family with a content of 14.8%. Incondensable gases account for a relative content of 13.2% and acids for 16.5%. In the acid family, the long-chain acids are the main compounds identified, e.g., undecanoic, hexadecanoic, and octadecanoic acids, with their contents being 3.9, 3.5, and 2.0%, respectively.

The families made up of ethers and hydrocarbon compounds are also produced in a significant amount (contents of 5.4% and 4.8%, respectively). Within ethers, 1-methoxy-9-octadecene and 1,1′-dimethoxy-9-octadecene have been identified and account for 3.9 and 1.4%, respectively. The hydrocarbon compounds are C_9-C_{18} aliphatic hydrocarbons (paraffins and olefins). The aromatic hydrocarbons identified have been toluene, ethylbenzene, and 1,2,3-trimethylbenzene, with the first one being the prevailing one with a content of 0.2%.

Concerning the deoxygenating activity of the dolomite, this catalyst lowers the content of oxygenated compounds from 98% (corresponding to thermal pyrolysis) to 93%, under the conditions tested (450 °C and a C/B ratio of 1). Therefore, it has a much lower deoxygenating capacity than the HZSM-5 zeolite (83% of oxygenate compounds), which is explained by the better features of the latter (acidity and porous structure) for this process.

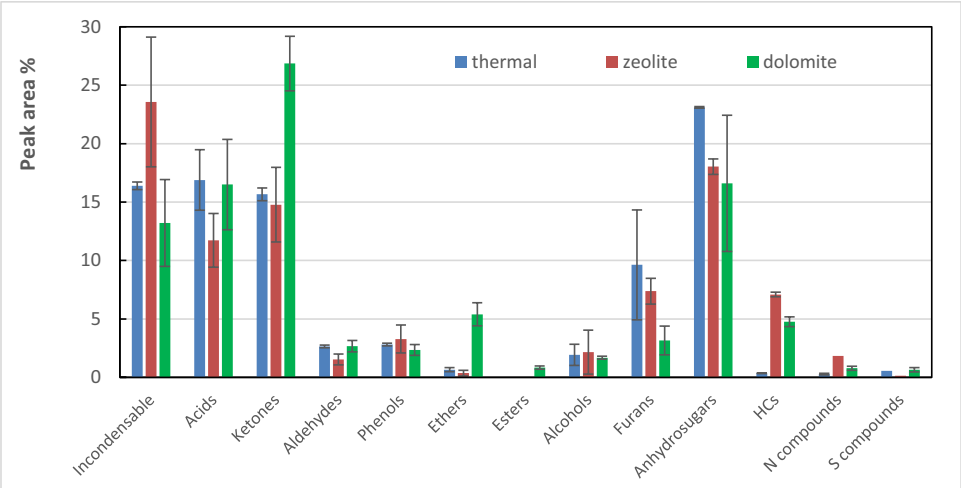

Fig. 11 Mean peak area percentages obtained in thermal and catalytic pyrolysis (on HZSM-5 and dolomite, C/B=1) at 450 °C

Comparison of thermal and catalytic pyrolysis on HZSM-5 and dolomite Given that the product distribution obtained is very different depending on whether a catalyst is used or not and on the type of catalyst used, Fig. 11 compares the product distributions obtained in the three situations (without catalyst and on HZSM-5 and dolomite catalyst) at a C/B ratio of 1 and 450 °C.

As observed, there are significant differences in the peak area percentages of the product families. Thus, a comparison of the results obtained in the thermal pyrolysis and those obtained on the dolomite shows that there is a large increase in the contents of ketones (from 15.7 to 26.9%), ethers (from 0.7 to 5.4%), and hydrocarbons (from 0.4 to 4.8%) when this catalyst is used, but a significant decrease in those of sugars (from 23.1 to 16.6%), with levoglucosan being the main compound, and specially furans (from 9.6 to 3.2%). The lower content of levoglucosan on dolomite or CaO has also been detected by other authors [22, 70].

A comparison of the results obtained in the catalytic pyrolysis on the dolomite and HZSM-5 zeolite shows that the major differences are the higher peak area percentages of incondensable gases, furans, and hydrocarbons obtained on the HZSM-5 zeolite. Aromatic hydrocarbons are the most abundant ones on the HZSM-5 zeolite, whereas non-aromatic hydrocarbons are the most abundant ones on the dolomite. It is noteworthy that the dolomite enhances the formation of ethers and especially of ketones.

4 Conclusions

The HZSM-5 zeolite is a suitable zeolite for the deoxygenation of the volatiles (bio-oil) generated in the pyrolysis of DPS biomass. This effect has been observed especially at 450 °C with a high C/B mass ratio (C/B =5) and leads to a significant increase in the content of incondensable gases (especially C_3-C_4 olefins) and a large increase in that of aromatic hydrocarbons. The most abundant compounds identified are benzene, toluene, xylenes, and polyaromatic hydrocarbons, such as naphthalene, fluorene, anthracene, and their derivatives. Simultaneously, a significant reduction in the content of acids, ketones, furans, and sugars has been determined, which is higher as the C/B ratio is higher. The acids and ketones are related to the acidity and instability of the bio-oil, and therefore, the decrease in their content improves the quality of the bio-oil. This deoxygenating activity of the HZSM-5 zeolite is due to its properties, such as acidity and porous structure (shape selectivity), which promote cracking and deoxygenation reactions, and so the formation of aromatic compounds.

In the case of the dolomite catalyst, a low deoxygenating activity has been determined due to its basic nature and low specific surface area. The most remarkable effect of this catalyst is the high content of ketones it allows obtaining. This is the consequence of ketonization reactions involving carboxylic acids, which are promoted by the dolomite catalyst to give linear ketones.

Acknowledgements The authors gratefully acknowledge the Tunisian Ministry of Higher Education and Scientific Research (MESRST), the Spanish Ministry of Science and Innovation (PID2019-107357RB-I00) (AEI/FEDER, UE), and the Basque Government (KK-2020/00107) for their financial support.

Author contribution MA, MO, and ABH designed the study. GB and MB conducted the experiments and collected the data. MA wrote the draft of the manuscript, while all other co-authors provided substantial feedback. All authors gave final approval for publication.

Funding Open Access funding provided thanks to the CRUE-CSIC agreement with Springer Nature. This project has received funding from the European Union's Horizon 2020 research and innovation

programme under the Marie Sklodowska-Curie grant agreement no. 823745.

Data availability Data and materials supporting the conclusions of the manuscript are available from the corresponding author on reasonable request.

Code availability Not applicable

Declarations

Competing interests The authors declare no competing interests.

References

1. Alper K, Tekin K, Karagöz S (2015) Pyrolysis of agricultural residues for bio-oil production. Clean Techn Environ Policy 17:211–223. https://doi.org/10.1007/s10098-014-0778-8
2. Ghouma I, Jeguirim M, Guizani C et al (2017) Pyrolysis of olive pomace: degradation kinetics, gaseous analysis and char characterization. Waste Biomass Valori 8:1689–1697. https://doi.org/10.1007/s12649-017-9919-8
3. Fang S, Gu W, Dai M et al (2018) A study on microwave-assisted fast co-pyrolysis of chlorella and tire in the N_2 and CO_2 atmospheres. Bioresour Technol 250:821–827. https://doi.org/10.1016/j.biortech.2017.11.080
4. Hernando H, Hernández-Giménez AM, Ochoa-Hernández C et al (2018) Engineering the acidity and accessibility of the zeolite ZSM-5 for efficient bio-oil upgrading in catalytic pyrolysis of lignocellulose. Green Chem 20:3499–3511. https://doi.org/10.1039/c8gc01722k
5. Hertzog J, Carré V, Jia L et al (2018) Catalytic fast pyrolysis of biomass over microporous and hierarchical zeolites: characterization of heavy products. ACS Sustain Chem Eng 6:4717–4728. https://doi.org/10.1021/acssuschemeng.7b03837
6. Serrano DP, Aguado J, Escola JM (2012) Developing advanced catalysts for the conversion of polyolefinic waste plastics into fuels and chemicals. ACS Catal 2:1924–1941. https://doi.org/10.1021/cs3003403
7. St M, Azhari NJ, Ilmi T, Kadj GTM (2022) Hierarchical zeolite for biomass conversion to biofuel: a review. Fuel 309:122119. https://doi.org/10.1016/j.fuel.2021.122119
8. Elordi G, Olazar M, Aguado R, Lopez G, Arabiourrutia M, Bilbao J (2007) Catalytic pyrolysis of high density polyethylene in a conical spouted bed reactor. J Anal Appl Pyrolysis 79:450–459. https://doi.org/10.1016/j.jaap.2006.11.010
9. Miskolczi N, Juzsakova T, Sója J (2019) Preparation and application of metal loaded ZSM-5 and y-zeolite catalysts for thermo-catalytic pyrolysis of real end of life vehicle plastics waste. J Energy Inst 92:118–127. https://doi.org/10.1016/j.joei.2017.10.017
10. Mihalcik DJ, Mullen CA, Boateng AA (2011) Screening acidic zeolites for catalytic fast pyrolysis of biomass and its components. J Anal Appl Pyrolysis 92:224–232. https://doi.org/10.1016/j.jaap.2011.06.001
11. Iliopoulou EF, Stefanidis SD, Kalogiannis KG et al (2012) Catalytic upgrading of biomass pyrolysis vapors using transition metal-modified ZSM-5 zeolite. Appl Catal B Environ 127:281–290. https://doi.org/10.1016/j.apcatb.2012.08.030
12. Park HJ, Jeon JK, Suh DJ, Suh YW, Heo HS, Park YK (2011) Catalytic vapor cracking for improvement of bio-oil quality. Catal Surv Asia 15:161–180. https://doi.org/10.1007/s10563-011-9119-7
13. Corma A, Huber GW, Sauvanaud L, Connor PO (2010) Processing biomass-derived oxygenates in the oil refinery: catalytic cracking (FCC) reaction pathways and role of catalyst. J Catal 247:307–327. https://doi.org/10.1016/j.jcat.2007.01.023
14. Gayubo AG, Aguayo T, Atutxa A, Aguado R (2004) Kinetics, catalysis, and reaction engineering Transformation of oxygenate components of biomass pyrolysis oil on a HZSM-5 zeolite. I. Alcohols and phenols. Ind Eng Chem Res 43:2610–2618. https://doi.org/10.1021/ie030791o
15. Demirbas A, Al-Sasi BO, Nizami AS (2016) Conversion of waste tires to liquid products via sodium carbonate catalytic pyrolysis. Energy Sources, Part A: Recover Util Environ Eff 38:2487–2493. https://doi.org/10.1080/15567036.2015.1052598
16. Lin X, Zhang Z, Zhang Z et al (2018) Catalytic fast pyrolysis of a wood-plastic composite with metal oxides as catalysts. Waste Manag 79:38–47. https://doi.org/10.1016/j.wasman.2018.07.021
17. Fernandez E, Santamaria L, Artetxe M, Amutio M, Arregi A, Lopez G, Bilbao J, Olazar M (2021) In line upgrading of biomass fast pyrolysis products using low-cost catalyst. Fuel 296(4):120682. https://doi.org/10.1016/j.fuel.2021.120682
18. Aljbour SH (2018) Catalytic pyrolysis of olive cake and domestic waste for biofuel production. Energy Sources, Part A: Recov, Util Environ Effects 40(23):2785–2791. https://doi.org/10.1080/15567036.2018.1511649
19. Aljeradat RA, Aljbour SH, Jarrah NA (2021) Natural minerals as potential catalysts for the pyrolysis of date kernels: effect of catalysts on products yield and bio-oil quality. Energy Sources, Part A: Recov Util Environ Effect. Published online. https://doi.org/10.1080/15567036.2021.2003485
20. Berrueco C, Montané D, Matas Güell B, del Alamo G (2014) Effect of temperature and dolomite on tar formation during gasification of torrefied biomass in a pressurized fluidized bed. Energy 66:849–859. https://doi.org/10.1016/j.energy.2013.12.035
21. Cortazar M, Lopez G, Alvarez J, Amutio M, Bilbao J, Olazar M (2019) Behaviour of primary catalysts in the biomass steam gasification in a fountain confined spouted bed. Fuel 253:1446–1456. https://doi.org/10.1016/j.fuel.2019.05.094
22. Ly HV, Lim DH, Sim JW et al (2018) Catalytic pyrolysis of tulip tree (Liriodendron) in bubbling fluidized-bed reactor for upgrading bio-oil using dolomite catalyst. Energy 162:564–575. https://doi.org/10.1016/j.energy.2018.08.001
23. Valle B, Aramburu B, Santiviago C et al (2014) Upgrading of bio-oil in a continuous process with dolomite catalyst. Energy Fuel 28:6419–6428. https://doi.org/10.1021/ef501600f
24. Mysore H, Prabhakara BEA, Brem G (2021) Role of dolomite as an in-situ CO_2 sorbent and deoxygenation catalyst in fast pyrolysis of beechwood in a bench scale fluidized bed reactor. Fuel Process Technol 224:107029. https://doi.org/10.1016/j.fuproc.2021.107029
25. Ghnimi S, Umer S, Karimb A, Kamal-Eldina A (2017) Date fruit (Phoenix dactylifera L.): an underutilized food seeking industrial

valorization. NFS J 6:1–10. https://doi.org/10.1016/j.nfs.2016.12.001
26. El May Y, Jeguirim M, Dorge S, Trouvé G, Said R (2012) Study on the thermal behavior of different date palm residues: characterization and devolatilization kinetics under inert and oxidative atmospheres. Energy August 44(1):702–709. https://doi.org/10.1016/j.energy.2012.05.022
27. Rahman MS, Kasapis S, Al-Kharusi NSZ, Al-Marhubi IM, Khan AJ (2007) Composition characterisation and thermal transition of date pits powders. J Food Eng 80(1):1–10. https://doi.org/10.1016/j.jfoodeng.2006.04.030
28. Adeosun AM, Oni SO, Ighodaro OM, Durosinlorun OH, Oyedele OM (2016) Minerals and free radical scavenging profiles of Phoenix dactilyfera L. seed extract. J Taibah Univ Med Sci 11(1):1–6. https://doi.org/10.1016/j.jtumed.2015.11.006
29. Ourradi H, Ennahli S, Viuda Martos M, Hernadez F, Dilorenzo C, Hssaini L, Elantari A, Hanine H (2021) Proximate composition of polyphenolic, phytochemical, antioxidant activity content and lipid profiles of date palm seeds oils (Phoenix dactylifera L.). J Agric Food Res 6:100217. https://doi.org/10.1016/j.jafr.2021.100217
30. Ogungbenro AE, Quang DV, Al-Ali KA, Vega LF, Abu-Zahra Mohammad RM (2020) Synthesis and characterization of activated carbon from biomass date seeds for carbon dioxide adsorption. J Environ Chem Eng 8(5):104257. https://doi.org/10.1016/j.jece.2020.104257
31. Ogungbenro AE, Quang DV, Al-Ali KA, Vega LF, Abu-Zahra Mohammad RM (2018) Physical synthesis and characterization of activated carbon from date seeds for CO_2 capture. J Environ Chem Eng 6(4):4245–4252. https://doi.org/10.1016/j.jece.2018.06.030
32. Habib HM, Ibrahim WH (2009) Nutritional quality evaluation of eighteen date pit varieties. Int J Food Sci Nutr 60(1):99–111. https://doi.org/10.1080/09637480802314639
33. Bensidhom G, Arabiourrutia M, Ben Hassen Trabelsi A et al (2021) Fast pyrolysis of date palm biomass using Py-GCMS. J Energy Inst 99:229–239. https://doi.org/10.1016/j.joei.2021.09.012
34. Sun X, Sun RC, Tomkinson J, Baird MS (2003) Preparation of sugarcane bagasse hemicellulosic succinates using NBS as a catalyst. Carbohydr Polym 53:483–495. https://doi.org/10.1016/S0144-8617(03)00150-4
35. Alvarez J, Hooshdaran B, Cortazar M, Amutio M, Lopez G, Freire FB, Haghshenasfard M, Hosseini SH, Olazar M (2018) Valorization of citrus wastes by fast pyrolysis in a conical spouted bed reactor. Fuel 224:111–120. https://doi.org/10.1016/j.fuel.2018.03.028
36. Wang S, Dai G, Yang H, Luo Z (2017) Lignocellulosic biomass pyrolysis mechanism: a state-of-the-art review. Prog Energy Combust Sci 62:33–86. https://doi.org/10.1016/j.pecs.2017.05.004
37. Yildiz G, Lathouwers T, Toraman HE et al (2014) Catalytic fast pyrolysis of pine wood: effect of successive catalyst regeneration. Energy Fuel 28(7):4560–4572. https://doi.org/10.1021/ef500636c
38. Anderson BD, Rytting JH, Higuchi T (1979) Influence of self association on the solubility of phenol in isooctane and cyclohexane. J Am Chem Soc 101(18):5194–5197. https://doi.org/10.1021/ja00512a014
39. Huynh VN, Dang NT, Truong TT, Van T (2021) Catalytic upgrading and enhancing the combustion characteristics of pyrolysis oil. Int J Green Energy 18(12):1277–1288. https://doi.org/10.1080/15435075.2021.1904403
40. Thangalazhy-Gopakumar S, Adhikari S, Chattanathan SA, Gupta RB (2012) Catalytic pyrolysis of green algae for hydrocarbon production using H(+)ZSM-5 catalyst. Bioresour Technol 118:150–157. https://doi.org/10.1016/j.biortech.2012.05.080
41. Garba MU, Musa U, Olugbenga AG, Mohammad YS, Yahaya M, Ibrahim AA (2018) Catalytic upgrading of bio-oil from bagasse: thermogravimetric analysis and fixed bed pyrolysis. Beni-suef Univ J Basic Appl Sci 7(4):776–781. https://doi.org/10.1016/j.bjbas.2018.11.004
42. Vitolo S, Bresci B, Seggiani M, Gallo MG (2001) Catalytic upgrading of pyrolytic oils over HZSM-5 zeolite: behavior of the catalyst when used in repeated upgrading-regenerating cycles. Fuel 80(1):17–26. https://doi.org/10.1016/S0016-2361(00)00063-6
43. Mentzel UV, Holm MS (2011) Utilization of biomass: conversion of model compounds to hydrocarbons over zeolite H-ZSM-5. Appl Catal A Gen 396:59–67. https://doi.org/10.1016/j.apcata.2011.01.040
44. Carlson TR, Vispute TP, Huber GW (2008) Green gasoline by catalytic fast pyrolysis of solid biomass derived compounds. Chem Sus Chem 1:397–400. https://doi.org/10.1002/cssc.200800018
45. Shahsavari S, Sadrameli SM (2020) Production of renewable aromatics and heterocycles by catalytic pyrolysis of biomass resources using rhenium and tin promoted ZSM-5 zeolite catalysts. Process Saf Environ Prot 141:305–320. https://doi.org/10.1016/j.psep.2020.04.023
46. Adjaye JD, Bakhshi NN (1995) Production of hydrocarbons by catalytic upgrading of a fast pyrolysis bio-oil. Part I: conversion over various catalysts. Fuel Process Technol 45:161–183. https://doi.org/10.1016/0378-3820(95)00034-5
47. Dong C, Zhang Z, Lu Q, Yang Y (2012) Characteristics and mechanism study of analytical fast pyrolysis of poplar wood. Energy Convers Manag 57:49–59. https://doi.org/10.1016/j.enconman.2011.12.012
48. Collard FX, Blin J (2014) A review on pyrolysis of biomass constituents: mechanisms and composition of the products obtained from the conversion of cellulose, hemicelluloses and lignin. Renew Sust Energ Rev 38:594–608. https://doi.org/10.1016/j.rser.2014.06.013
49. Foster AJ, Jae J, Cheng Y et al (2012) Optimizing the aromatic yield and distribution from catalytic fast pyrolysis of biomass over ZSM-5. Appl Catal A, Gen 423–424:154–161. https://doi.org/10.1016/j.apcata.2012.02.030
50. Liu R, Sarker M, Rahman MM et al (2020) Multi-scale complexities of solid acid catalysts in the catalytic fast pyrolysis of biomass for bio-oil production–a review. Prog Energy Combust Sci 80:100852. https://doi.org/10.1016/j.pecs.2020.100852
51. Lazaridis PA, Fotopoulos AP, Karakoulia SA et al (2018) Catalytic fast pyrolysis of kraft lignin with conventional, mesoporous and nanosized ZSM-5 zeolite for the production of alkyl-phenols and aromatics. Front Chem 6:295. https://doi.org/10.3389/fchem.2018.00295
52. Adjaye JD, Bakhshi NN (1995) Catalytic conversion of a biomass-derived oil to fuels and chemicals I: model compound studies and reaction pathways. Biomass Bioenergy 8(3):131–149. https://doi.org/10.1016/0961-9534(95)00018-3
53. Jeon M-J, Jeon J-K, Suh DJ et al (2013) Catalytic pyrolysis of biomass components over mesoporous catalysts using Py-GC/MS. Catal Today 204:170–178. https://doi.org/10.1016/j.cattod.2012.07.039
54. Cheng Y, Huber GW (2012) Production of targeted aromatics by using Diels – Alder classes of reactions. Green Chem 14:3114–3125. https://doi.org/10.1039/C2GC35767D
55. Nikbin N, Do PT, Caratzoulas S et al (2013) A DFT study of the acid-catalyzed conversion of 2, 5-dimethylfuran and ethylene to p-xylene. J Catal 297:35–43. https://doi.org/10.1016/j.jcat.2012.09.017
56. Vichaphund S, Aht-ong D, Sricharoenchaikul V (2014) Catalytic upgrading pyrolysis vapors of Jatropha waste using metal

promoted ZSM-5 catalysts: an analytical PY-GC/MS. Renew Energy 65:70–77. https://doi.org/10.1016/j.renene.2013.07.016
57. Anand V, Sunjeev V, Vinu R (2016) Catalytic fast pyrolysis of *Arthrospira platensis* (spirulina) algae using zeolites. J Anal Appl Pyrolysis 118:298–307. https://doi.org/10.1016/j.jaap.2016.02.013
58. Setter C, Silva FTM, Assis MR et al (2020) Slow pyrolysis of coffee husk briquettes: characterization of the solid and liquid fractions. Fuel 261:116420. https://doi.org/10.1016/j.fuel.2019.116420
59. Choudhary VR, Panjala D, Banerjee S (2002) Aromatization of propene and n-butene over H-galloaluminosilicate (ZSM-5 type) zeolite. Appl Catal A Gen 231:243–251. https://doi.org/10.1016/S0926-860X(02)00061-3
60. Lukyanov DB, Gnep NS, Guisnet MR (1994) Kinetic modeling of ethene and propene aromatization over HZSM-5 and GaHZSM-5. Ind Eng Chem Res 33(2):223–234. https://doi.org/10.1021/ie00026a008
61. Kim B-S, Kim Y-M, Jae J et al (2015) Pyrolysis and catalytic upgrading of Citrus unshiu peel. Bioresour Technol 194:312–319. https://doi.org/10.1016/j.biortech.2015.07.035
62. Nguyen TS, Zabeti M, Lefferts L et al (2013) Catalytic upgrading of biomass pyrolysis vapours using faujasite zeolite catalysts. Biomass Bioenergy 48:100–110. https://doi.org/10.1016/j.biombioe.2012.10.024
63. Stephanidis S, Nitsos C, Kalogiannis K et al (2011) Catalytic upgrading of lignocellulosic biomass pyrolysis vapours: effect of hydrothermal pre-treatment of biomass. Catal Today 167:37–45. https://doi.org/10.1016/j.cattod.2010.12.049
64. Zhang H, Xiao R, Jin B, Shen D, Chen R, Xiao G (2013) Catalytic fast pyrolysis of straw biomass in an internally interconnected fluidized bed to produce aromatics and olefins: effect of different catalysts. Bioresour Technol 137:82–87. https://doi.org/10.1016/j.biortech.2013.03.031
65. Chen X, Chen Y, Yang H et al (2017) Fast pyrolysis of cotton stalk biomass using calcium oxide. Bioresour Technol 233:15–20. https://doi.org/10.1016/j.biortech.2017.02.070
66. Charusiri W, Vitidsant T (2017) Upgrading bio-oil produced from the catalytic pyrolysis of sugarcane (*Saccharum officinarum L*) straw using calcined dolomite. Sustain Chem Pharm 6:114–123. https://doi.org/10.1016/j.scp.2017.10.005
67. Zhou M, Li J, Wang K, Xia H, Xu J, Jiang J (2017) Selective conversion of furfural to cyclopentanone over CNT-supported Cu based catalysts: model reaction for upgrading of bio-oil. Fuel 202:1–11. https://doi.org/10.1016/j.fuel.2017.03.046
68. Pham TN, Sooknoi T, Crossley S, Resasco DE (2013) Ketonization of carboxylic acids : mechanisms, catalysts, and implications for biomass conversion. ACS Catal 3:2456–2473. https://doi.org/10.1021/cs400501h
69. Pham TN, Shi D, Resasco DE (2014) Evaluating strategies for catalytic upgrading of pyrolysis oil in liquid phase. Appl Catal B Environ 145:10–23. https://doi.org/10.1016/j.apcatb.2013.01.002
70. Lu Q, Zhang ZF, Dong CQ, Zhu XF (2010) Catalytic upgrading of biomass fast pyrolysis vapors with nano metal oxides: an analytical Py-GC/MS study. Energies 3:1805–1820. https://doi.org/10.3390/en3111805